ARTICLE
Journal of Cellular Biochemistry 116:1205–1212 (2015)

Journal of Cellular Biochemistry

Isolation, Characterization and Cardiac Differentiation of Human Thymus Tissue Derived Mesenchymal Stromal Cells

Ze Bang Lin, Bo Qian, Yu Zhong Yang, Kai Zhou, Jian Sun, Xu Ming Mo, and Kai Hong Wu*

Department of Cardiothoracic Surgery, Nanjing Children's Hospital, Nanjing Medical University, Nanjing, China

ABSTRACT

Mesenchymal stromal cells (MSCs) are promising candidate donor cells for replacement of cardiomyocyte loss during ischemia and in vitro generation of myocardial tissue. We have successfully isolated MSCs from the discarded neonatal thymus gland during cardiac surgery. The thymus MSCs were characterized by cell-surface antigen expression. These cells have high ability for proliferation and are able to differentiate into osteoblasts and adipocytes in vitro. For cardiac differentiation, the cells were divided into 3 groups: untreated control; 5-azacytidine group and sequential exposure to 5-azacytidine, bone morphogenetic protein 4, and basic fibroblast growth factor. Thymus MSCs showed a fibrolast-like morphology and some differentiated cells increased in size, formed a ball-like appearance over time and spontaneously contracting cells were observed in sequential exposure group. Immunostaining studies, cardiac specific genes/protein expression confirmed the cardiomyocyte phenotype of the differentiated cells. These results demonstrate that thymus MSCs can be a promising cellular source for cardiac cell therapy and tissue engineering. J. Cell. Biochem. 116: 1205–1212, 2015.

KEY WORDS: THYMUS TISSUE; MESENCHYMAL STROMAL CELLS; DIFFERENTIATION; CARDIOMYOCYTE

The heart's limited regenerative capacity make acquired heart failure and congenital heart disease significant and essentially incurable. Recent advances in cell therapy and cardiac tissue engineering using stem cells, especially the use of MSCs show great promise for future therapy of cardiovascular diseases [Phinney, 2012; Rodrigo et al., 2013]. The main properties of MSCs include their high potential for self-renewal and their capacity to differentiate into other lineages under specific in vitro culture conditions. MSCs can be isolated from various tissues including bone marrow, adipose tissue, muscle, dermis, and umbilical cord tissue [Wu et al., 2011]. The presence of MSCs in human fetal thymus as a surgical waste was also demonstrated recently [Mouiseddine et al., 2008; Siepe et al., 2009].

In this study, the MSCs were successfully isolated from neonatal thymus tissue by enzymatic digestion. The morphology and growth characteristics of thymus MSCs were similar to that of human umbilical cord derived MSCs (UC-MSCs) [Wu et al., 2009]. After sequential exposure to 5-azacytidine (5-aza), bone morphogenetic protein 4 (BMP4), and basic fibroblast growth factor (bFGF), the thymus MSCs differentiated into beating cardiomyoctes in vitro. Immunostaining revealed the typical striation and palestaining pattern of the sarcomeres. Cardiac specific genes/protein expression confirmed the cardiomyocyte phenotype of the differentiated cells. These results suggest that thymus MSCs might be a promising cellular source for cardiac cell therapy and tissue engineering.

MATERIALS AND METHODS

ISOLATION OF THYMUS MSCS

With the consent of the parents, fresh thymus tissue was collected as surgical waste from neonate undergoing cardiac surgery according to the regulations of Nanjing Medical University Research Ethics Committee and the stem cells were isolated immediately. After removal of blood vessels, the thymus was washed extensively with Dulbecco's modified Eagle's medium with low glucose (DMEM-LG/F-12, DF12; Gibco). Then, the tissue was minced into 1 mm^3 pieces and treated with 2 mg/ml collagenase IV (Sigma), and further digested with 0.25% trypsin (Sigma). Fetal bovine serum (FBS) was added to the mesenchymal tissues to neutralize the excess trypsin.

Conflicts of interests: none.

Grant sponsor: National Natural Science Foundation of China; Grant number: 81100114; Grant sponsor: Nanjing Medical Science and Technique Development Foundation; Grant number: QYK11152, QRX11011.

*Correspondence to: Dr. Kai Hong Wu, Department of Cardiothoracic Surgery, Nanjing Children's Hospital, Nanjing Medical University, 72 Guangzhou Road, Nanjing, 210008, China. E-mail: pumcwu@aliyun.com

Manuscript Received: 1 February 2014; Manuscript Accepted: 18 December 2014

Accepted manuscript online in Wiley Online Library (wileyonlinelibrary.com): 23 December 2014

DOI 10.1002/jcb.25072 • © 2014 Wiley Periodicals, Inc.

The digested mixture was then passed through a 100 μm filter to obtain cell suspensions. Finally, the cells were plated on 60-mm culture dishes and allowed to proliferate in DF12 medium, supplemented with 10% FBS, 10ng/ml epidermal growth factor (EGF; Pepro Tech), 100U penicillin/streptomycin (Sigma) and cultured at 37°C in a 5% CO_2 humidified incubator. After 3 days of culture, nonadherent cells were removed, and adherent cells were washed and incubated until confluence in DF12 medium. Medium was then changed every 2 or 3 days and serially expanded. UC-MSCs were used as a control in this study.

COLONY-FORMING UNIT-FIBROBLAST (CFU-F) ASSAY

The CFU-F assay was made as previously described [Castro-Malaspina et al., 1980] with some modifications. In brief, 1×10^6 thymus MSCs or UC- MSCs were seeded in T-25 flasks, and cultured at 37°C in a 5% CO_2 humidified incubator. The medium was changed every 3 days. For limiting dilution assay, the cells were seeded in six-well plates in 6 dilution steps: $1 \times 10^5/5 \times 10^4/2.5 \times 10^4/1.25 \times 10^4/6.25 \times 10^3/3.125 \times 10^3$ cells/well. The culture medium was changed every 3 days. The fibroblast colonies were counted on day 10 of culture. A colony was considered as a CFU-F when composed of more than 50 cells.

PROLIFERATION ASSAY

To study the doubling time, thymus MSCs and UC-MSCs from p1 to p10 were seeded in T-25 flasks. The cells were harvested daily and enumerated for 6 consecutive days. Three sets of cultures were done. The mean of the counts was calculated and plotted against culture time to generate a growth curve. The mean doubling time was obtained by the formula: TD = tplg2/(lgNt-lgN0). N0: the initial cell number, Nt is the cell harvest number at time (t, in hours). The doubling time of cells from P1 to P10 was calculated.

SENESCENCE ASSAY

Senescence assay was performed with thymus MSCs using senescence β-galactosidase (β-gal) staining kit (Cell Signaling Technologies) according to the manufacturer's protocol. Cells from different passages were observed for development of blue color under a microscope (Nikon).

SURFACE PHENOTYPE CHARACTERIZATION

The cell surface markers of thymus MSCs were analyzed by flow cytometry. After trypsinization, the detached cells were washed and resuspended in phosphate buffered saline (PBS). Approximately 10^6 cells were incubated with antibodies against fluorescein isothiocyanate (FITC)-conjugated CD31, CD34, CD90 CD106, and HLA-ABC, phycoerythrin (PE)-conjugated CD29, CD45, CD73, CD105, HLA-DR (All from Becton Dickinson). All incubations were performed at room temperature for 20 min. After incubation cells were washed with PBS containing 0.1%BSA. Finally, the cells were assayed in a FACS flow cytometer (Becton Dickinson).

DIFFERENTIATION ANALYSIS

To investigate the multi-directional differentiation of the isolated thymus MSCs, osteogenic differentiation and adipogenic differentiation were performed. For osteogenic differentiation, thymus and UC-MSCs from passages (p4–10) were incubated in α-MEM supplemented with 10% FBS, dexamethasone (0.1μmol/L), ascorbic acid (0.2mmol/L), and β-glycerophosphate(10mmol/L) (all from Sigma) for 2 weeks. Then the cells were stained with von Kossa to reveal osteogenic differentiation. For adipogenic differentiation, the cells were induced for 3 weeks in α-MEM supplemented with 10% FBS, hydrocortisone (0.5μmol/L), isobutylmethylxanthine(0.5 mmol/L), and indomethacin (50μg/ml) (all from Sigma). At the end of the culture, the cells were fixed and stained with fresh Oil red-O solution (Sigma). The osteogeneic specific genes, osteopontin (OPN) and collagen type I (COL-I), as well as the adipogenic specific genes, lipoprotein lipase (LPL) and peroxisome proliferators activated receptor gamma (PPAR-γ) were further detected by reverse transcriptase polymerase chain reaction (RT-PCR) as described below. The sequences of the appropriate primers are listed in Table 1.

CARDIAC DIFFERENTIATION

For cardiac differentiation, the thymus MSCs (p4–10) were divided into 3 groups: control group; 5-aza group; sequential group: sequential exposure to 5-aza (Sigma), BMP4, (R&D system) and b-FGF (R&D) with defined media as shown in Figure 4A. Briefly, cells were seeded into 6-well plates at a density of 10,000 cells/cm^2 in DF-12 supplemented with 10% FBS and 10 ng/ml EGF. The medium was changed every other day, when the monolayer of cells reached 90% to 100% confluence, which is referred to as day 0 when the medium was replaced with Roswell Park Memorial Institute medium (RPMI) 1640 basal medium (Invitrogen) plus B27 without insulin supplement (Invitrogen) containing 5 μmol/L 5-aza. Twenty-four hours later, the medium was changed with the same medium as day 1 supplemented

TABLE 1. Primer Sequences Used for RT-PCR

Gene	Forward primer	Reverse primer	Size (bp)
OPN	CTAGGCATCACCTGTGCCATACC	CAGTGACCAGTTCATCAGATTCATC	330
COL-I	ATCAAGGTCTACTGCAACAT	CAGGATCGGAACCTTCGCTT	178
LPL	ATGGAGAGCAAAGCCCTGCTC	TACAGGGCGGCCACAAGTTTT	298
PPAR-γ	GTCTCACAATGCCATCAGGTT	TTCAGCTGGTCGATATCACT	90
NKX2.5	GCGATTATGCAGCGTGCAATGAGT	AACATAAATACGGGTGGGTGCGTG	220
α- actin	CCAGGCACTGTGGAAAGG	CACGATGGATGGGAAGAC	286
MLC-2α	ATTGAGCTTCTCCCCAAAGAG	GCAGACCTGAGGGAGACCTAC	135
α-MHC	GCAGACCATCAAGGACCT	GTTGGCCTGTTCCTCCGCC	310
MEF2C	GCAGACGATTCAGTAGGT	CCAGTGGCAGAAGATTA	211
Troponin	GCGAAGCAGGAGATGGAG	TGCCACGCAGGTCATAGA	250
GAPDH	GTCAGTGGTGGACCTGACCT	CACCACCCTGTTGCTGTAGC	255

with 10 ng/ml BMP4 and 10 ng/ml bFGF for another 3 days. At day 4, the medium was changed to RPMI plus B27 complete supplement (Invitrogen), and the medium was changed every 2 to 3 days. The cells were monitored daily by phase-contrast microscopy.

RT-PCR ANALYSIS

Total RNA was isolated from the cells and human heart tissue using Trizol reagent (Invitrogen) followed by phenol-chloroform extraction. RT-PCR was performed according to the manufacturer's instruction (Invitrogen) by using primers for the following genes, NKX2.5, cardiac α- actin, myosin light chain (MLC-2α), myosin heavy chain (α-MHC), myocyte enhancer factor 2C(MEF2C), Troponin I, Glyceraldehyde 3-phosphate dehydrogenase (GAPDH) served as an internal control (Table 1).

IMMUNOSTAINING OF CARDIAC DIFFERENTIATION

Differentiated cells (day 30) were digested with 0.25% trypsin-EDTA, and the cells were plated on gelatin-coated coverslips for 3–5 days to allow full attachment. Cells were then fixed in 4% paraformaldehyde and incubated with primary antibodies: mouse anti-human myosin light chain (MLC-2α, Chemicon), anti-human cardiac sarcomeric α-actin (Chemicon), anti human cardiac Troponin T (cTnT, Newmarker). Secondary antibodies specific to the primary IgG isotype were used as needed. After the nuclei were counterstained with 4′,6-diamidino-2-phenylindole (DAPI, Invitrogen), immunofluorescence images were visualised and recorded using a confocal microscope (Leica Microsystems, GmbH).

WESTERN BLOT ANALYSIS OF CARDIAC DIFFERENTIATION

One well of a 6-well plate of each differentiated groups (day 30) was lysed with RIPA lysis buffer for western blotting (supplementary methods).

ELECTROPHYSIOLOGY

Action potentials (APs) were recorded from spontaneously beating cells as described [Zhang et al., 2009]. Briefly, microdissected beating areas were maintained in RPMI medium plus 10% FBS for 3 to 5 days before recording. The electrical activity of differentiated cardiomyocytes was measured using sharp microelectrodes (50–100 MΩ; 3 mol/L KCl) in a 37°C bath continuously perfused with Tyrode solution. Junction potentials and capacitance were nulled and data were acquired at 10 kHz using an AxoClamp2A amplifier and pClamp 9.2 software (Molecular Devices). Electrical field stimulation was performed using 2 platinum electrodes coupled to a Grass SD-9 stimulator.

STATISTICAL ANALYSIS

Data are presented as mean ± standard deviation. Statistical analysis was performed to analyze variance among groups by Student's *t*-test using SPSS statistical software. Results were considered statistically significant if statistical P values <0.05.

RESULTS

MORPHOLOGY AND GROWTH CHARACTERISTICS

When initially plated, the isolated cells appeared round-shaped, the cells were adherent, elongated, and spindle-shaped 48 h later (Fig. 1A). The sub-cultured cells showed a fibroblast-like morphology (Fig. 1B). The cell proliferation curves showed the frequency of CFU-F increased cell-seeding densities (Fig. 1C). The population doubling time of thymus MSCs was higher than that of UC-MSCs through P1 to P10, but with no statistical differences ($P > 0.05$). The thymus MSCs can be passaged more than 20 times, without visible changes in morphology, indicating the high proliferation potential of thymus MSCs, similar to that of UC-MSCs. However, the mean doubling time increased notably after P10 (Fig. 1D). Senescence is characterized by cell cycle arrest, telomere shortening and altered morphology. We did not detect much of senescence associated β-gal staining in thymus MSCs till passage 10; however, β-gal staining increased notably after P10 (Fig. 1E–G).

SURFACE PHENOTYPE CHARACTERIZATION

Flow cytometry analysis showed that the isolated cells highly expressed CD29, CD90, CD73, CD105, and HLA-ABC, but not CD31, CD34, CD45, CD106, and HLA-DR, similar to the FACS results of UC-MSCs and bone marrow derived MSCs (Fig. 2).

OSTEOGENIC AND ADIPOGENIC DIFFERENTIATION

When the cells were differentiated in osteogenic and adipogenic medium, they were positive for von Kossa (Fig. 3A, B) and Oil red staining respectively (Fig. 3C, D). To further confirm the osteogenic and adipogenic differentiation, the expression of osteogeneic specific genes, OPN and COL-I and adipogenic specific genes, LPLand PPAR-γ were analyzed by RT-PCR before and after induction. No expression of OPN and COL-I was found in thymus or UC-MSCs in basic culture conditions (before induction). After osteogenic induction, the cells expressed the mRNA of OPN and COL-I (Fig. 3E). No expression of LPL and PPAR-γ was found before induction. After adipogenic induction, the cells expressed the mRNA of LPL and PPAR-γ (Fig. 3F). For adipogenic differentiation, the differentiation ratio was 67–70% and there was no significant difference in the percentage of positive cells between UC-MSCs and thymus MSCs.

CARDIAC DIFFERENTIATION ANALYSIS

The thymus MSCs adhered to the plastic surface as short spindle-shaped cells 2 days after plating, and 2 or 3 days later, when the monolayer of cells reached 90% to 100% confluent, we started the differentiation with the addition of 5-aza and/or BMP4. After exposure to 5-aza and BMP4, a limited number of cells gradually increased in size, formed a ball-like appearance after induction in both 5-aza and sequential group (Fig. 4B, C). But, the beating cells were only found in sequential group. Immunostaining revealed that cardiac specific cTnT was strongly expressed in 5-aza and sequential group, but no expression in control group (Fig. 5A–C). We also calculated the percentage of the human cardiac cTnT positive cells to determine the cardiomyocytic differentiation rate of thymus MSCs. While thymus MSCs in untreated control group did not show any cTnT expression, approximately 27% of thymus MSCs became positive for cTnT antibody as a result of the 5-aza treatment and 40% in sequential group with BMP4 (Fig. 5D).

We confirmed the expression of cardiomyocyte related genes by RT-PCR. No expression of cardiac-specific genes was detected in control cells, but 5-Aza/BMP4 treatment strongly induced expression

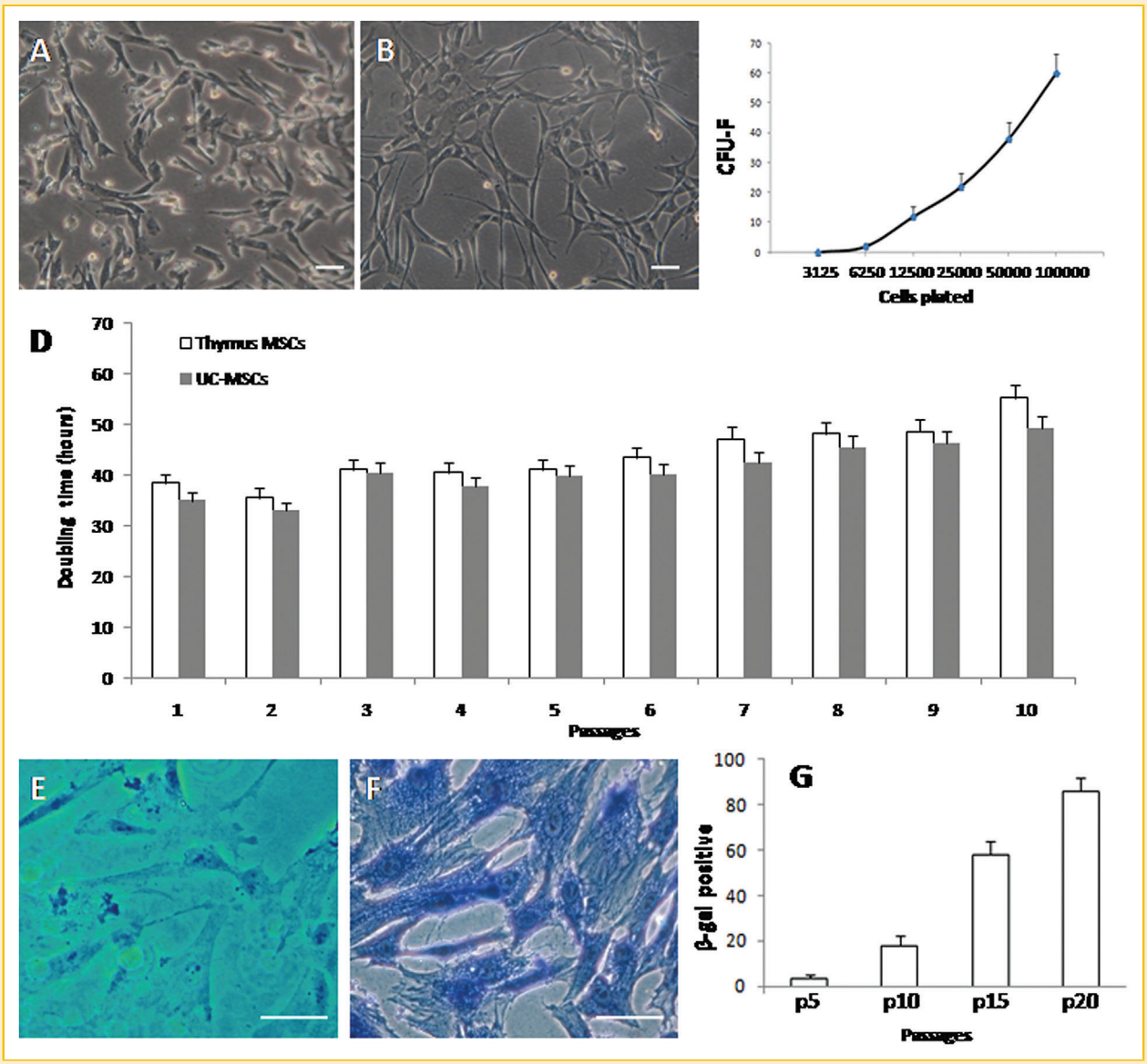

Fig. 1. The morphology, growth kinetics and senescence of thymus MSCs. A, Primary isolated cells (A) and sub-cultured stem cells (B) displayed a fibroblastic morphology. The frequency of CFU-F and the mean doubling time (P1 to P10) of thymus MSCs was similar to that of UC-MSCs (C–D). Senescence associated β- gal staining of thymus MSCs at p10 and p20 (E-F). β-gal staining increased notably after P10 (G).

of Nkx2.5, one of the earliest cardiac markers, and contractile proteins, α-sarcomeric actin, MLC-2α, and α-MHC, as well as the cardiomyocyte-related genes MEF2C and cTnI (Fig. 5E). To further verify the differentiation of thymus MSCs into cardiomyocytes, we evaluated cTnI proteins by western blot analysis. Density analysis of western blotting bands showed that the cTnI protein level in both groups was higher than that in the control group ($P < 0.01$, Fig. 5F), while the sequential exposure group with BMP4 was even higher than that in 5-aza group ($P < 0.01$).

IMMUNOSTAINING AND ELECTROPHYSIOLOGICAL TRACING

Immunocytochemistry revealed that a significant number of thymus MSCs in sequential exposure group with BMP4 were stained positive by the anti-human sarcomeric α-actin and MLC-2α antibody (Fig. 6A–D). Higher magnification view of the immunostaining clearly revealed the typical striation and palestaining pattern of the sarcomeres (Fig. 6E). The electrophysiological phenotype of differentiated cardiomyocytes was also investigated to assess the heterogeneity and function of cardiomyocytes. Sharp microelectrode recordings of spontaneous APs from differentiated cardiomyocytes revealed there were at least two types of distinguishable morphological APs: ventricular-like APs, which were the predominant form and atrial-like potentials (Fig. 6F).

DISCUSSION

MSCs are considered a promising candidate for replacement of cardiomyocyte loss during ischemia and in vitro generation of heart

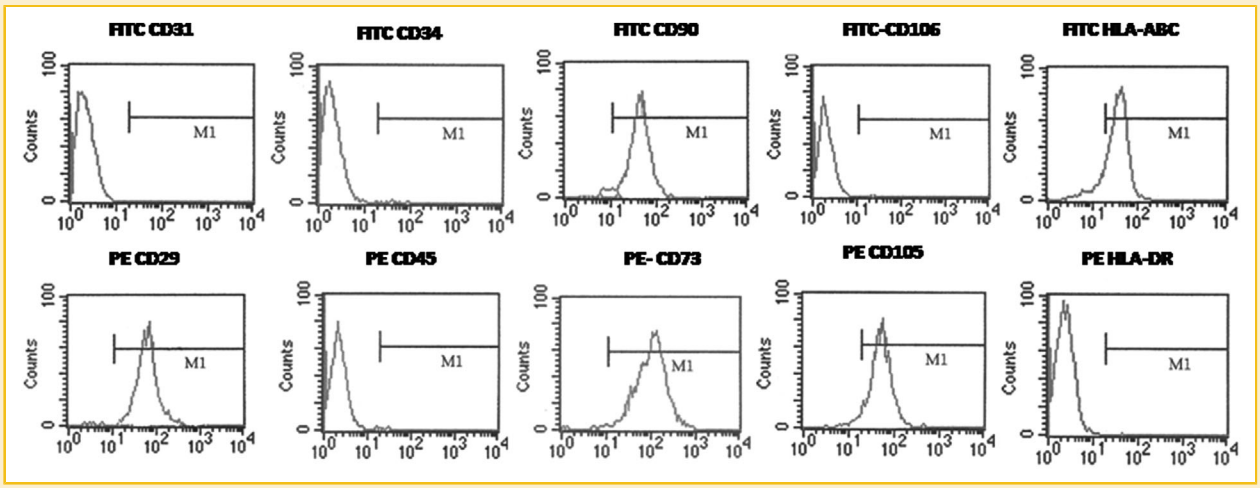

Fig. 2. Flow cytometry results of thymus MSCs. Data are representative of several independent experiments.

tissue [Wu et al., 2012]. Most of the research in cardiac cell therapy has been conducted using MSCs from bone marrow, however, MSCs are rare in adult human bone marrow and the number significantly decreases with age [Asumda and Chase, 2011; Yagi et al., 2013]. During neonatal cardiac surgery, the thymus gland of affected neonates is frequently excised to allow unrestricted access to the heart and great arteries[Sondergaard et al., 2010].

In the present study, we showed that MSCs could be isolated from the neonatal thymus gland. Thymus MSCs expressed a number of membrane molecules including CD29, CD73, CD90, CD105, they also presented a low expression of HLA-ABC and no expression of hematopoietic linage markers, like CD31, CD34, CD45, CD106, and HLA-DR, similar to the FACS results of UC-MSCs bone marrow derived MSCs [Wu et al., 2007; Wu et al., 2009]. Since MSCs possess a limited lifespan during in vitro culture, they finally undergo replicative senescence [Cheng et al., 2011; Alessio et al., 2013]. Based on senescence associated β-gal staining, very few senescent cells could be found before p10, and without visible changes in morphology, indicating the high proliferation potential of thymus MSCs.

Makino et al. first reported that bone marrow MSCs could differentiate into cardiomyocytes after exposure to 5-aza [Makino et al., 1999]. Nishiyama et al. and others suggested that cardiac microenvironment was important for obtaining functional cardiomyocytes [Nishiyama et al., 2007; Choi et al., 2010; Otaka et al., 2013]. In the present study, exposure to 5 μmol/L 5-aza could differentiate thymus MSCs into cardiomyocyte-like cells, but no beating cells were observed. However, when further treated with

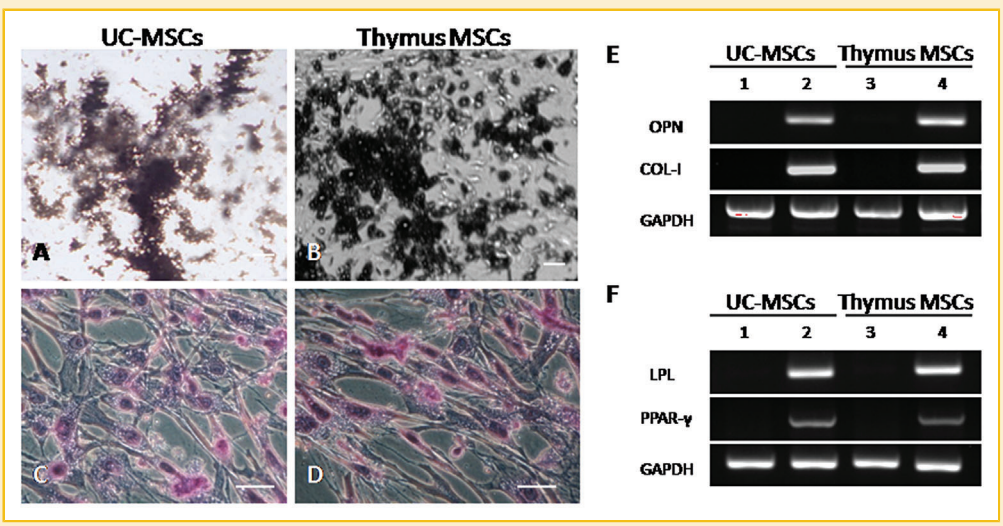

Fig. 3. Osteogenic and adipogenic differentiation. Osteogenic differentiation and adipogenic differentiation was evidenced by von Kossa staining (A–B) and oil-red O staining (C–D) in both UC-MSCs and thymus MSCs. E, Expression of OPN and COL-I after osteogenic lineage differentiation. 1,3: before induction; 2,4: two weeks after induction. F, Expression of LPL and PPAR-γ after adipogenic lineage differentiation. 1,3: before induction; 2,4: Three weeks after induction. Bar: 50 μm.

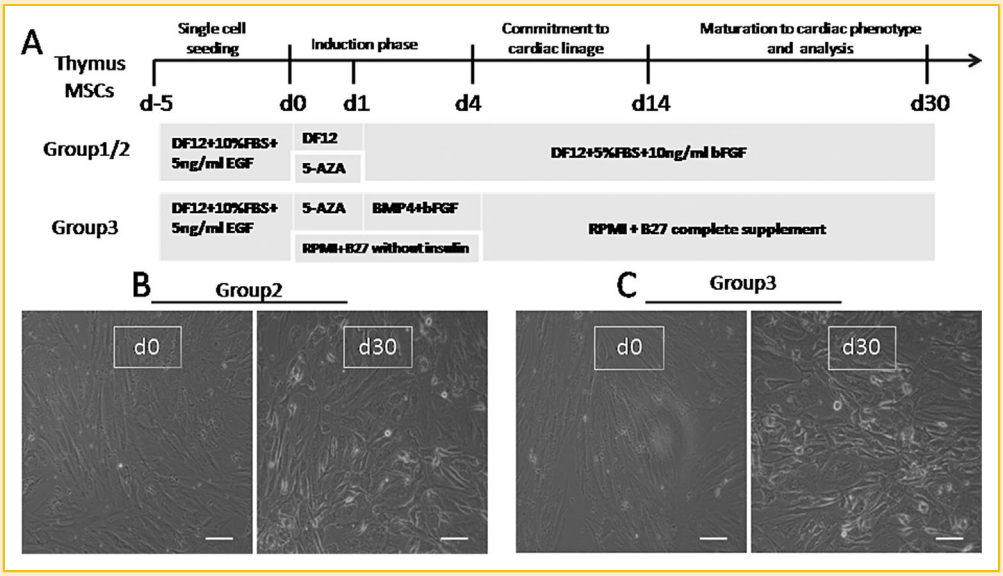

Fig. 4. Schematic of the cardiomyocyte differentiation protocol and the morphology changes during the differentiation process. A, Schematic of the cardiomyocyte differentiation protocol. B, C: Morphological changes of differentiated thymus MSCs in 5-AZA group and sequential exposure group. Bar: 100 μm.

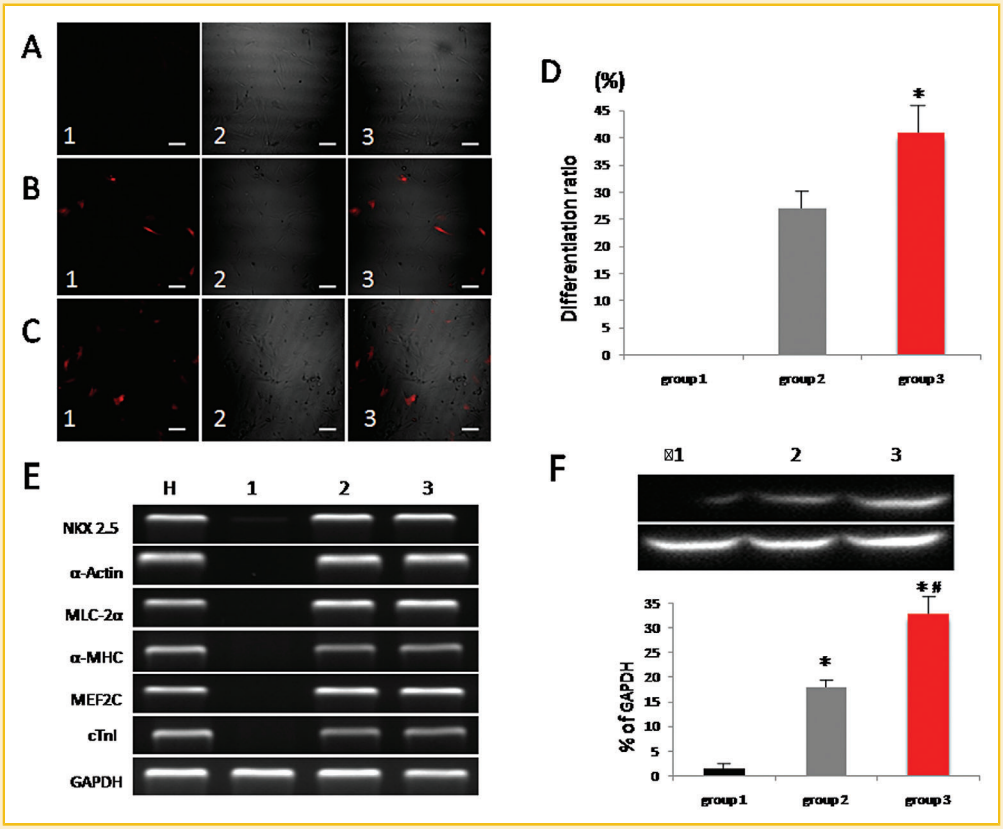

Fig. 5. Immunostaining and cardiac gene/protein expression of differentiated thymus MSCs. Detection of cTnT in 3 different groups (A, control, B, 5-aza group, C, sequential group). Representative images were presented for cardiac cTnT (panel 1), bright-field image (panel 2) and the overlay images (panel 3). Bar: 100 μm. The rate of differentiation was defined as the percentage of cTnT positive cells in the thymus MSCs. Measured data were averaged and shown (D). E, RT-PCR analysis of the expression of mRNA for cardiac-specific genes, including NKX 2.5, α-actin, MLC-2α, α-MHC, MEF2C, cTnI in control (1), 5-aza (2), and sequential group (3), human heart tissue served as a positive control (H), GAPDH was used as internal RT-PCR control. F, The expression levels of cTnI were determined by western blotting. Representative data from 3 independent groups are shown, * <0.01 versus Control group, # $P<0.01$ versus 5-aza group.

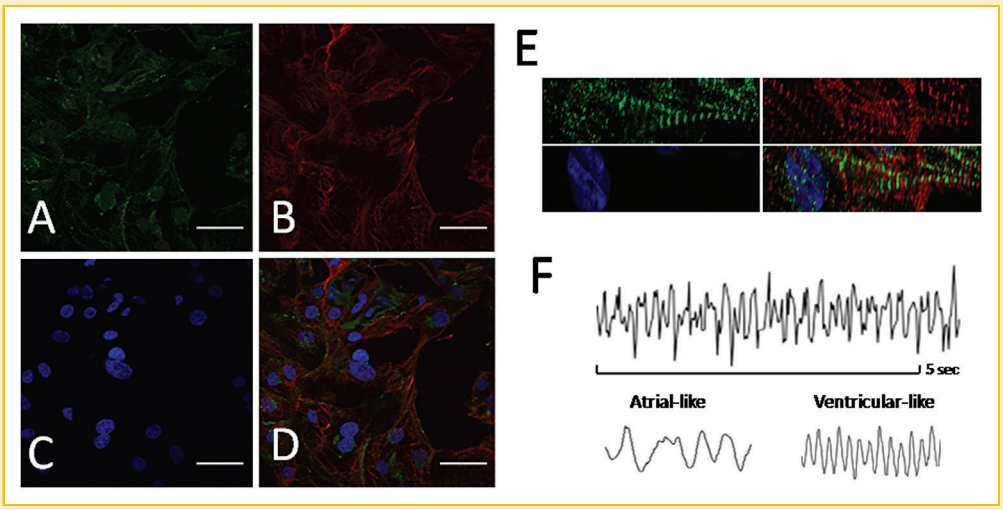

Fig. 6. Immunostaining and tracing of the action potentials of thymus MSCs differentiated in sequential exposure group. Significant numbers of differentiated thymus MSCs had sarcomeric α-actin (A) and MLC-2α, (B) in their cytoplasm. D, Overlay of A, B and DAPI staining (C). Bar: 50 μm. Sarcomeric α-actin, MLC-2α and merge of single cardiomyocyte are magnified in panel E. F, Representative microelectrode recordings of atrial-like and ventricular-like APs from thymus MSC-cardiomyocytes.

BMP4 and bFGF, spontaneous contracting cells were observed at day 14. Immunostaining showed that the differentiated cells were strongly positive for cardiac MLC-2α antibody. Compared to the differentiation efficiency of the thymus MSCs in the 5-aza group, a significant number of cells differentiated into cardiomyocytes after sequential exposure to 5-aza, BMP4, and bFGF. RT–PCR confirmed the gene expression of cardiomyocytes. Density analysis of western blotting bands showed that the cTnI protein level in the sequential exposure group with BMP4 was significantly higher than that in 5-aza group. One reason for this situation might be attributed to the fact that there is a variety of additional factors necessary to promote the differentiation of thymus MSCs to cardiomyocytes.

Immunocytochemistry revealed that a significant number of thymus MSCs in sequential exposure group were positive for cardiac specific α-actin and MLC-2α. Higher magnification view of the immunostaining revealed the typical striation and palestaining pattern of the sarcomeres. Furthermore, generated contracting cardiomyocytes showed physiologically cardiomyocyte-specific APs with long duration. Our results suggested that BMP4 was critical in the differentiation of thymus MSCs into cardiomyocytes and the additional factors might be essential for obtaining beating functional cardiomyocytes because the chemical agent alone might not be enough to differentiate thymus MSCs into beating cardiomyocytes.

In summary, our work revalidates previous studies indicating possible generation of functional cardiomyocytes using human thymus MSCs. Although the present study is not intended to describe a novel method for in vitro generation of cardiomyoytes, it is conceivable that functional cardiomyocytes can be generated after sequential exposure to 5-aza, BMP4 and bFGF with defined media, and similar methodology may contribute to generation of transplantable cardiac tissue in the future. However, the underlying molecular mechanisms by which thymus MSCs differentiate into contracting cardiomyocytes require extensive further research. The model described herein will serve as a platform for such future studies, and the knowledge obtained will provide novel therapeutic strategies for the treatment of heart disease.

REFERENCES

Alessio N, Bohn W, Rauchberger V, Rizzolio F, Cipollaro M, Rosemann M, Irmler M, Beckers J, Giordano A, Galderisi U. 2013. Silencing of RB1 but not of RB2/P130 induces cellular senescence and impairs the differentiation potential of human mesenchymal stem cells. Cell Mol Life Sci 70:1637–1651.

Asumda FZ, Chase PB. 2011. Age-related changes in rat bone-marrow mesenchymal stem cell plasticity. BMC Cell Biol 12:44.

Castro-Malaspina H, Gay RE, Resnick G, Kapoor N, Meyers P, Chiarieri D, McKenzie S, Broxmeyer HE, Moore MA. 1980. Characterization of human bone marrow fibroblast colony-forming cells (CFU-F) and their progeny. Blood 56:289–301.

Cheng H, Qiu L, Ma J, Zhang H, Cheng M, Li W, Zhao X, Liu K. 2011. Replicative senescence of human bone marrow and umbilical cord derived mesenchymal stem cells and their differentiation to adipocytes and osteoblasts. Mol Biol Rep 38:5161–5168.

Choi YS, Dusting GJ, Stubbs S, Arunothayaraj S, Han XL, Collas P, Morrison WA, Dilley RJ. 2010. Differentiation of human adipose-derived stem cells into beating cardiomyocytes. J Cell Mol Med 14:878–889.

Makino S, Fukuda K, Miyoshi S, Konishi F, Kodama H, Pan J, Sano M, Takahashi T, Hori S, Abe H, Hata J, Umezawa A, Ogawa S. 1999. Cardiomyocytes can be generated from marrow stromal cells in vitro. J Clin Invest 103:697–705.

Mouiseddine M, Mathieu N, Stefani J, Demarquay C, Bertho JM. 2008. Characterization and histological localization of multipotent mesenchymal stromal cells in the human postnatal thymus. Stem Cells Dev 17:1165–1174.

Nishiyama N, Miyoshi S, Hida N, Uyama T, Okamoto K, Ikegami Y, Miyado K, Segawa K, Terai M, Sakamoto M, Ogawa S, Umezawa A. 2007. The significant cardiomyogenic potential of human umbilical cord blood-derived mesenchymal stem cells in vitro. Stem Cells 25:2017–2024.

Otaka S, Nagura S, Koike C, Okabe M, Yoshida T, Fathy M, Yanagi K, Misaki T, Nikaido T. 2013. Selective isolation of nanog-positive human amniotic mesenchymal cells and differentiation into cardiomyocytes. Cell Reprogram 15:80–91.

Phinney DG. 2012. Functional heterogeneity of mesenchymal stem cells: Implications for cell therapy. J Cell Biochem 113:2806–2812.

Rodrigo SF, van Ramshorst J, Hoogslag GE, Boden H, Velders MA, Cannegieter SC, Roelofs H, Al Younis I, Dibbets-Schneider P, Fibbe WE, Zwaginga JJ, Bax JJ, Schalij MJ, Beeres SL, Atsma DE. 2013. Intramyocardial injection of autologous bone marrow-derived ex vivo expanded mesenchymal stem cells in acute myocardial infarction patients is feasible and safe up to 5 years of follow-up. J Cardiovasc Transl Res 6:816–825.

Siepe M, Thomsen AR, Duerkopp N, Krause U, Forster K, Hezel P, Beyersdorf F, Schlensak C, Sudkamp NP, Bosse R, Niemeyer P. 2009. Human neonatal thymus-derived mesenchymal stromal cells: Characterization, differentiation, and immunomodulatory properties. Tissue Eng Part A 15:1787–1796.

Sondergaard CS, Hodonsky CJ, Khait L, Shaw J, Sarkar B, Birla R, Bove E, Nolta J, Si MS. 2010. Human thymus mesenchymal stromal cells augment force production in self-organized cardiac tissue. Ann Thorac Surg 90:796–803.discussion 803–4.

Wu KH, Mo XM, Han ZC, Zhou B. 2011. Stem cell engraftment and survival in the ischemic heart. Ann Thorac Surg 92:1917–1925.

Wu KH, Mo XM, Han ZC, Zhou B. 2012. Cardiac cell therapy: Preconditioning effects in cell-delivery strategies. Cytotherapy 14:260–266.

Wu KH, Mo XM, Zhou B, Lu SH, Yang SG, Liu YL, Han ZC. 2009. Cardiac potential of stem cells from whole human umbilical cord tissue. J Cell Biochem 107:926–932.

Wu KH, Zhou B, Lu SH, Feng B, Yang SG, Du WT, Gu DS, Han ZC, Liu YL. 2007. In vitro and in vivo differentiation of human umbilical cord derived stem cells into endothelial cells. J Cell Biochem 100:608–616.

Yagi H, Tan J, Tuan RS. 2013. Polyphenols suppress hydrogen peroxide-induced oxidative stress in human bone-marrow derived mesenchymal stem cells. J Cell Biochem 114:1163–1173.

Zhang J, Wilson GF, Soerens AG, Koonce CH, Yu J, Palecek SP, Thomson JA, Kamp TJ. 2009. Functional cardiomyocytes derived from human induced pluripotent stem cells. Circ Res 104:e30–e41.

SUPPORTING INFORMATION

Additional supporting information may be found in the online version of this article at the publisher's web-site.